# Optical properties of light emitting diodes with a cascading plasmonic grating

**Chih-Ming Wang,[1,*] Yao-Lin Tsai,[1] Sheng-Han Tu,[2,3] Chien-Chieh Lee,[4] Cheng-Huang Kuo,[5] and Jenq-Yang Chang[2, 4]**

*[1]Institute of Opto-electronic Engineering, National Dong Hwa University, Hualien, 97401 Taiwan, China*
*[2]Department of Optics and Photonics, National Central University, Jhongli, 32001 Taiwan, China*
*[3] Genesis Photonics Inc. No.5 Dali 3rd RD., Tainan Science-Based Industrial Park, 74144, Taiwan China*
*[4]Center of Optics, National Central University, Jhongli, 32001 Taiwan, China*
*[5]Institute of Lighting and Energy Photonics, National Chiao Tung University, Tainan County 71150, Taiwan, China*
** wangcm@mail.ndhu.edu.tw*

**Abstract:** In this paper, the polarization dependent optical properties of InGaN/GaN multi-quantum wells (MQWs) LED with cascading plasmonic gratings are investigated using an angle-resolved photoluminescence (ARPL) spectrometer. The plasmonic gratings consist of two Ag gratings with a half-pitch displacement. The ARPL spectra of the TE-TM state present a broadband emission with resonance dips occasioned by the SP resonance while the TM-TE state presents resonance peaks with low sideband emission. The resonance properties can be tuned by modifying the geometric parameters of the plasmonic grating. The ARPL spectrum of the LED sample with pure GaN 1D grating is also measured and discussed. The investigated plasmonics LED represents resonance optical properties different from the conventional surface relief LED, which can be used in special applications.



**OCIS codes:** (240.6680) Surface plasmons; LED; light extraction.

## References and links

1. J. B. Kim, S. M. Kim, Y. W. Kim, S. K. Kang, S. R. Jeon, N. Hwang, Y. J. Choi, and C. S. Chung, "Light Extraction Enhancement of GaN-Based Light-Emitting Diodes Using Volcano-Shaped Patterned Sapphire Substrates," Jpn. J. Appl. Phys. **49**(4), 042102 (2010).
2. C. H. Lin, C. Y. Chen, D. M. Yeh, and C. C. Yang, "Light Extraction Enhancement of a GaN-Based Light-Emitting Diode Through Grating-Patterned Photoelectrochemical Surface Etching With Phase Mask Interferometry," IEEE Photon. Technol. Lett. **22**(9), 640–642 (2010).
3. C. Wiesmann, K. Bergenek, N. Linder, and U. T. Schwarz, "Photonic crystal LEDs - designing light extraction," Laser Photon. Rev. **3**(3), 262–286 (2009).
4. C. Y. Huang, H. M. Ku, and S. Chao, "Light extraction enhancement for InGaN/GaN LED by three dimensional auto-cloned photonics crystal," Opt. Express **17**(26), 23702–23711 (2009).
5. J. M. Hwang, K. F. Lee, and H. L. Hwang, "Optical and electrical properties of GaN micron-scale light-emitting diode," J. Phys. Chem. Solids **69**(2-3), 752–758 (2008).
6. Z. Gong, E. Gu, S. R. Jin, D. Massoubre, B. Guilhabert, H. X. Zhang, M. D. Dawson, V. Poher, G. T. Kennedy, P. M. W. French, and M. A. A. Neil, "Efficient flip-chip InGaN micro-pixellated light-emitting diode arrays: promising candidates for micro-displays and colour conversion," J. Phys. **41**, 094002 (2008).
7. W. S. Wong, T. Sands, and N. W. Cheung, "Damage-free separation of GaN thin films from sapphire substrates," Appl. Phys. Lett. **72**(5), 599–601 (1998).
8. V. Haerle, B. Hahn, S. Kaiser, A. Weimar, S. Bader, F. Eberhard, A. Plössl, and D. Eisert, "High brightness LEDs for general lighting application Using the new ThinGaN Technology," Phys. Status Solidi **201**(12), 2736–2739 (2004).
9. L. C. Chen, and Y. M. Ho, "Ag and zinc oxide-doped indium oxide ohmic contacts to p-type GaN for flip-chip LED applications," J. Phys. **40**, 6514–6517 (2007).
10. C. F. Shen, S. J. Chang, W. S. Chen, T. K. Ko, C. T. Kuo, and S. C. Shei, "Nitride-based high-power flip-chip LED with double-side patterned sapphire substrate," IEEE Photon. Technol. Lett. **19**(10), 780–782 (2007).
11. I. Gontijo, M. Boroditsky, E. Yablonovitch, S. Keller, U. K. Mishra, and S. P. DenBaars, "Coupling of InGaN quantum-well photoluminescence to silver surface plasmons," Phys. Rev. B **60**(16), 11564–11567 (1999).
12. W. L. Barnes, "Electromagnetic crystals for surface plasmon polaritons and the extraction of light from emissive devices," J. Lightwave Technol. **17**(11), 2170–2182 (1999).

#136890 - $15.00 USD Received 19 Oct 2010; revised 9 Nov 2010; accepted 12 Nov 2010; published 22 Nov 2010

13. S. Gianordoli, R. Hainberger, A. Köck, N. Finger, E. Gornik, C. Hanke, and L. Korte, "Optimization of the emission characteristics of light emitting diodes by surface plasmons and surface waveguide modes," Appl. Phys. Lett. **77**(15), 2295–2297 (2000).
14. J. Vuckovic, M. Loncar, and A. Scherer, "Surface plasmon enhanced light-emitting diode," IEEE J. Quant. Electron. **36**(10), 1131–1144 (2000).
15. P. A. Hobson, S. Wedge, J. A. E. Wasey, I. Sage, and W. L. Barnes, "Surface plasmon mediated emission from organic light emitting diodes," Adv. Mater. **14**(19), 1393–1396 (2002).
16. A. Neogi, C. W. Lee, H. O. Everitt, T. Kuroda, A. Tackeuchi, and E. Yablonovitch, "Enhancement of spontaneous recombination rate in a quantum well by resonant surface plasmon coupling," Phys. Rev. B **66**(15), 153305 (2002).
17. K. Okamoto, I. Niki, A. Shvartser, Y. Narukawa, T. Mukai, and A. Scherer, "Surface-plasmon-enhanced light emitters based on InGaN quantum wells," Nat. Mater. **3**(9), 601–605 (2004).
18. K. Okamoto, I. Niki, A. Scherer, Y. Narukawa, T. Mukai, and Y. Kawakami, "Surface plasmon enhanced spontaneous emission rate of InGaN/GaN quantum wells probed by time-resolved photoluminescence spectroscopy," Appl. Phys. Lett. **87**(7), 071102 (2005).
19. M. K. Kwon, J. Y. Kim, B. H. Kim, I. K. Park, C. Y. Cho, C. C. Byeon, and S. J. Park, "Surface-Plasmon-Enhanced Light-Emitting Diodes," Adv. Mater. **20**(7), 1253–1257 (2008).
20. K. Okamoto, and Y. Kawakami, "High-Efficiency InGaN/GaN Light Emitters Based on Nanophotonics and Plasmonics," IEEE J. Sel. Top. Quantum Electron. **15**(4), 1199–1209 (2009).
21. E. D. Palik ed., *Handbook of optical constants of solids* (Academic Press, San Diego 1985).
22. J. Moreland, A. Adams, and P. K. Hansma, "Efficiency of light emission from surface plasmons," Phys. Rev. B **25**(4), 2297–2300 (1982).
23. P. T. Worthing, and W. L. Barnes, "Efficient coupling of surface Plasmon polaritons to radiation using a bi-grating," Appl. Phys. Lett. **79**(19), 3035–3037 (2001).
24. A. David, C. Meier, R. Sharma, F. S. Diana, S. P. DenBaars, E. Hu, S. Nakamura, C. Weisbuch, and H. Benisty, Photonic bands in two-dimensionally patterned multimode GaN waveguides for light extraction," Appl. Phys. Lett. **87**(10), 101107 (2005).

## 1. Introduction

GaN is one of the most promising semiconductors for optoelectronic applications in the blue spectral region. The commercialization of bright blue and green light emitting diodes (LED) based on group-III nitrides is a milestone in the competition for blue light sources which are important for fabricating full-color displays.

However, the high refractive index of GaN prohibits light beyond a critical angle from being extracted due to the total internal reflection. A large fraction of the light generated is trapped inside the LED and absorbed by non-radiative absorption centers. The internal absorption loss of the LED additionally increases as its chip size is enlarged, and as a consequence, much more heat is generated. Versatile approaches have been proposed and demonstrated to improve the output efficiency of III-nitride-based LEDs, such as surface texturing of LED and/or substrate [1,2], photonic crystals (PhCs) [3,4], micrometer-scale LEDs (μ-LEDs) [5,6], thin GaN structures [7,8], and flip-chip packaging [9,10]. Since Okamoto et al. reported a huge 14-fold PL enhancement and a 6.8-fold IQE enhancement of InGaN quantum wells (QWs) by QW-SP coupling, the SP-enhanced LED, plasmonic LEDs have attracted great interests. Through controlling the energy transfer between QW emitters and SPs, it has been demonstrated that the density of states, the spontaneous emission rate and internal quantum efficiency in the LED can be significantly increased [11–18]. In order to arouse the effects of plasmonic LED, the distance between the metal layer and the QWs is critical. The distance should be shorter than the penetration depth of the SP fringing field in to the GaN. In addition, rough metallic surfaces are needed to scatter the SP into free space. For instance, nano particles, i.e. the use of localized surface Plasmon (LSP), are applied and present similar results [19]. It has been found that IQEs can reach almost 100% efficiency under the best matching condition between the emission wavelength and the SP frequency. It is expected that full color devices and natural white LEDs can be created by using only InGaN/GaN material by combining plasmonic structures [20].

In this study, we investigate the optical properties of InGaN/GaN QWs LEDs with two cascading plasmonic gratings. The plasmonic gratings consist of two Ag gratings with a half-pitch displacement. The polarization dependent ARPL spectra of the plasmonic LED are measured. The investigated plasmonics LED represents resonance optical properties different from the conventional surface relief LED, which can be used as special applications.

#136890 - $15.00 USD Received 19 Oct 2010; revised 9 Nov 2010; accepted 12 Nov 2010; published 22 Nov 2010

## 2. Fabrication of cascading plasmonic LED

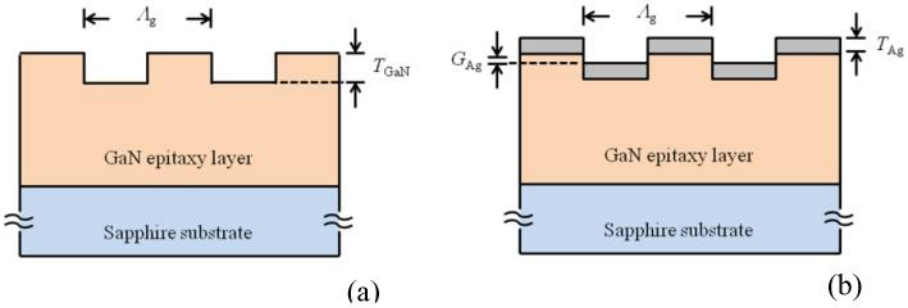


Fig. 1. Schematic representation of InGaN/GaN LED (a) with pure GaN grating and (b) with cascading plasmonic gratings.

Figure 1 shows a schematic representation of the investigated structure, the InGaN/GaN MQWs LED with surface relief structures. The LED wafer used in this study was grown using metal organic chemical vapor deposition (MOCVD) technology. The GaN film is grown on the 2-inch diameter and (001) orientation sapphire surface. The total thickness of the GaN epitaxy layer, including the buffer layer, n-GaN, MQWs and p-GaN and so on, is about 5μm. The peak wavelength of the GaN wafer is designed to be 460nm. An 1D grating was fabricated on the GaN film by using e-beam lithography and inductively coupled plasma (ICP) dry etching techniques. The grating periodicity is denoted by $\Lambda_g$. Two samples with periods of 0.3μm and 0.5μm are made. Figure 2 shows the scanning electron microscope (SEM) pictures of the fabricated GaN grating. The etching depth of the sample is measured by using Atomic force microscopy (AFM) and listed in Table 1. After the GaN grating is made, an Ag film with a thickness of 50nm is deposited by using E-gun evaporator. Finally, two cascaded Ag gratings with a half-pith displacement were fabricated. The gap between the two gratings is denoted as $G_{Ag}$. There is no Ag coating on the sidewall of the grating which is measured by using SEM.

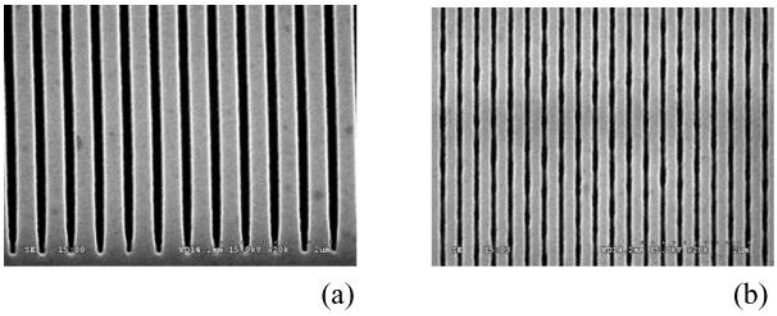


Fig. 2. SEM pictures of the 1D GaN grating with a period of (a) 0.3μm and (b) 0.5μm, respectively.

In addition, the distance between the topmost QWs and the bottommost of silver grating is 20nm which is within the penetration depth for SP at the Ag/GaN interface. The theoretical penetration depth ($Z$) of the SP fringing field into the semiconductor is given by $Z = \lambda/2\pi[(\varepsilon'_{GaN}-\varepsilon'_{Ag})/\varepsilon'^{2}_{GaN}]^{1/2}$ where $\varepsilon'_{GaN}$ and $\varepsilon'_{Ag}$ are the real parts of the dielectric constants of the GaN and Ag, respectively [19]. The theoretical penetration depth is $Z$ = 42nm for $\lambda$ = 460nm. Therefore, the topmost QW can be coupled by the SP. However, most of the QW layers are out of the penetration depth of SP at the Ag/GaN interface.

#136890 - $15.00 USD Received 19 Oct 2010; revised 9 Nov 2010; accepted 12 Nov 2010; published 22 Nov 2010

**Table 1. Geometric parameters of the fabricated samples**

| | Period | Etching depth | Ag thickness | Gap |
|---|---|---|---|---|
| Sample 1 | 0.3μm | 180nm | 50nm | 130nm |
| Sample 2 | 0.5μm | 180nm | 50nm | 130nm |

## 3. Description of the angle-resolved photoluminescence spectrum measurement

A schematic representation of the angle-resolved photoluminescence spectrum (ARPL) setup is shown in Fig. 3. The pumping source of the ARPL spectrum is a diode laser with a wavelength of 405nm and an output power of 17mW. The pumping light normally impinges on the sample from the sapphire substrate to the grating structure. The polarization of the laser is controlled by a linear polarizer. Two orthogonal polarization states, TE and TM, are used through all of the ARPL measurements. Here, TE is defined as the electric field parallel to the grating grooves and TM is defined as the magnetic field parallel to the grating grooves. The emission light is collected by a multimode fiber with a core diameter of 600μm. The polar emission angle is denoted as $\theta$. The working distance between the fiber and the rotation center of the ARPL spectrometer is 5cm. Similar to the pumping source; the polarization-dependent PL signal can be measured by placing an analyzer (i.e. a linear polarizer) in front of the multimode fiber. The analyzer is controlled so that it remains normal to the polarization state of the pumping source. When the pumping source is TE-polarized, the output fiber collects the TM-polarized PL signal. We call this type of PL measurement TE-TM state. When the pumping source is TM-polarized, the output fiber collects the TE-polarized PL signal. We call this type of PL measurement the TM-TE state. The emissions of the structure are recorded as a function of both incident wavelength and incident angle using a computer controlled rotating stage to support the structure being examined.

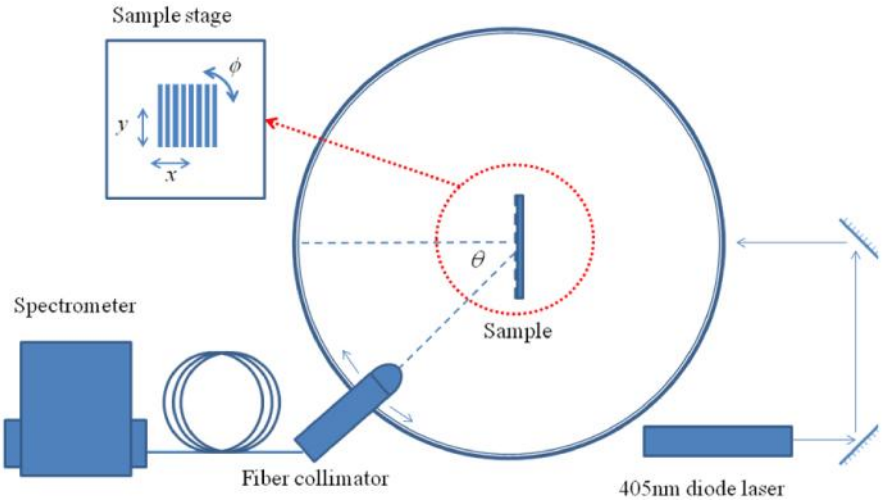


Fig. 3. Experimental setup for measuring the ARPL of nanostructured samples. Inset shows definitions for θ: collecting angle of the fiber, ϕ: sample orientation, and x/y movement directions.

Although the pumping source is polarized, the excited PL signal presents a spontaneous emission nature which is unpolarized. Therefore, the pumping source can be shuttered by using the cross polarizer set. The PL signal can still be detected due to the random polarization.

## 4. Angle-resolved photoluminescence spectrum of TE-TM mode

Figure 4 shows the ARPL spectra of the TE-TM state for grating periods 0.3μm and 0.5μm, respectively. The dark regions correspond to low emittance. Owing to the fact that the

#136890 - $15.00 USD Received 19 Oct 2010; revised 9 Nov 2010; accepted 12 Nov 2010; published 22 Nov 2010

pumping source normally impinges on the symmetric structure, the ARPL spectrum for $\theta = 0°$ to $\theta = 90°$ is identical to that for $\theta = 0°$ to $\theta = -90°$. Thus, only half of the ARPL spectrum is shown. Because the polarization of the 405nm pumping source is parallel to the grating grooves, it cannot arouse the SP coupling effect between the metallic grating and the pumping source. However, the emission light is unpolarized. Thus, parts of the unpolarized light may still couple with the SP. The blue lines show the grating coupled SP dispersion relation of the GaN/Ag interface, i.e. the moment conservation equation, $k_{sp} = k_0((\varepsilon_m \times \varepsilon_d)/(\varepsilon_m + \varepsilon_d))^{1/2} = k_x + m(2\pi/\Lambda_g)$, where $k_{sp}$ is the wave vector of the SPPs; $\varepsilon_m$ and $\varepsilon_d$ is the permittivity of Ag and air, respectively; $k_x$ is the parallel wave vector of the emission light; $2\pi/\Lambda_g$ is the reciprocal lattice vector of the Ag grating; and $m$ is an integer. The dispersive-complex permittivity for Ag ($\varepsilon_m$) can be referred to in reference [21]. The dashed and dotted lines represent $m = 1$, $m = 2$ and, respectively.

It can be seen in Fig. 4(a) that there is a broad emission peak at 450nm. There is a dark fringe tilted from $\theta = -21°$ to $\theta = -30°$ for the emission wavelength at 430nm to 470nm. This fringe has a fair agreement with the SPP dispersion at Ag/Air interface for $m = 1$. Owing to the fact that the pumping source is TE-polarized, the generation of SPP is not excited by the pumping source. This reveals that parts of the emission light are coupled to SPP at the Ag/Air interface and dissipate during propagation which leads to a dark fringe. In general, if nothing is done to recover power lost to SP modes, they then contribute to the nonradiative loss. However, some methods have been proposed to couple SPs to produce useful radiation [22,23]. As the grating period is increased from 0.3μm to 0.5μm, the dark fringe is tilted from $\theta = -12°$ to $\theta = -5°$ for the emission wavelength from 430nm to 470nm. This fringe has a fair agreement with the SPP dispersion at the Ag/Air interface for $m = 1$ as well. The theoretical SPP dispersion at the Ag/Air interface for $m = 2$ is also shown in Fig. 4(b). However, owing to the fact that the emission light is faint, the corresponding dark line is barely observable in the experimental results.

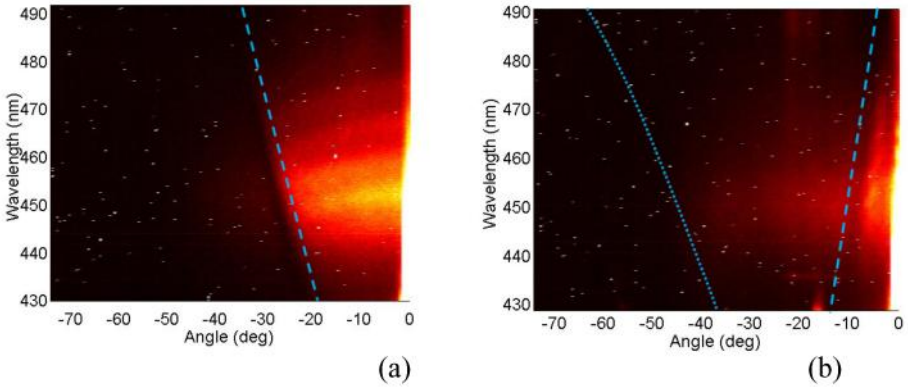


Fig. 4. TE-TM mode ARPL spectra of InGaN/GaN MQWs with a cascading plasmonic grating for grating periods of (a) 0.3μm and (b) 0.5μm, respectively.

## 5. Angle-resolved photoluminescence spectrum for the TM-TE mode

For the TM-TE state, the ARPL spectrum of the plasmonic LED shows a clear resonance peak red-shift from 453.3nm to 456.8nm as the collecting angle increases from –35° to –37° for a period of 0.3μm as shown in Fig. 5(a). The resonance wavelength shifts 1.8nm/deg. Owing to the LED being covered by plasmonic structures, most of the off-resonance light, no matter whether for the leakage or bound modes, is back reflected. When the period is 0.5μm, two resonance peaks can be found as shown in Fig. 5(b). One resonance peak red-shifts from 448.8nm to 452.3nm as the collecting angle increases from $\theta = -14°$ to $\theta = -16°$ while the other one blue-shifts from 462.7nm to 458.0nm as the polar emission angle increases from $\theta = -35°$ to $\theta = -37°$. The wavelength shift of the red-shift and blue-shift peak is 1.8nm/deg and

#136890 - $15.00 USD Received 19 Oct 2010; revised 9 Nov 2010; accepted 12 Nov 2010; published 22 Nov 2010

2.4nm/deg, respectively. When the polar emission angle is fixed as $\theta = -14°$, the resonance wavelength of the plasmonic LED with a period of 0.5μm is 449nm and the full width half maximum is 6nm, i.e. the Q value of the resonance peak is 75. These dispersion curves neither conserve with the SP dispersion for the Ag/Air interface nor for the Ag/GaN one. The slope of the dispersion curve for 0.3μm is more gradual than for the 0.5μm case. In other words, the effective index for 0.3μm is larger than that for 0.5μm. A straightforward idea to explain this is that one of waveguide modes inside of the GaN film is coupled out by the grating, i.e. the band folding of the free-photon dispersion. However, the thickness of the GaN thin film layer is about 5μm which can support tens of TE and TM waveguide modes. In such a thick planar waveguide, the propagation constants of TE and TM modes are close to each other. In addition, the higher order branch of the folded dispersion line is close to the lower order one. Consequently, there should be tens of folded free-photon dispersion lines. However, only single dispersion line is observed in the spectral range from 430nm to 490nm. Therefore, the sharp resonance peak is not a waveguide mode otherwise similar experimental results should be presented for the TE-TM mode.

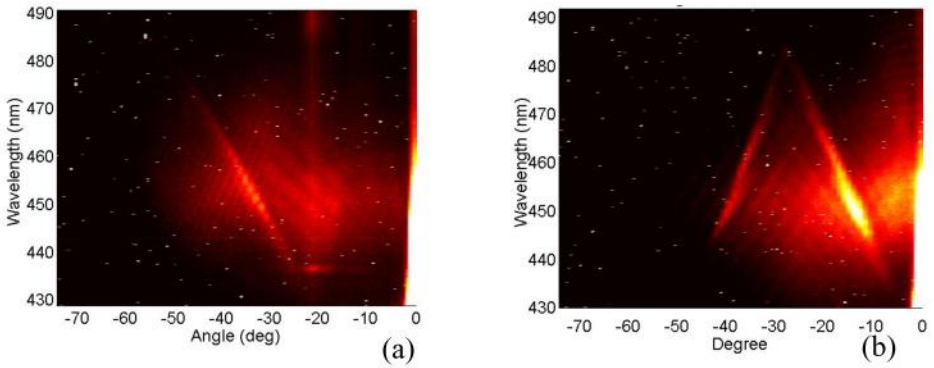


Fig. 5. TM-TE mode ARPL spectra of InGaN/GaN MQWs with a cascading plasmonic grating for grating periods of (a) 0.3μm and (b) 0.5μm, respectively.

In order to be compared with the optical properties of the plasmonic LED, the ARPL spectrum of a pure GaN grating, i.e. without being coated with a Ag layer, is also measured. As shown in Fig. 6, there are three kinds of resonance features in the ARPL spectrum. The broadest periodic oscillating peaks arise from the interference between forward (Air/GaN interface) and back (GaN/sapphire) scattered modes is the Fabry-Perot (FP) resonance. These FP resonances are not observed in the plasmonic samples. The narrower oscillating peaks, marked with a blue dashed circle are due to the waveguide modes inside the GaN waveguide coupled out by the grating [24]. The nature and number of the optical modes in the GaN layer is dictated solely by the geometric parameters and optical constants of the LED structures. In the case where waveguide modes can be coupled out, this depends not only on the available modes but also the corresponding distribution of the waveguide modes themselves and the modulation of the grating. The peaks of the coupled out waveguide modes are close because the propagation constants of the neighboring modes are similar due to the nature of a thick planar waveguide. It also shows resonance peaks with dispersion properties identical to the plasmonic LEDs for both 0.3μm and 0.5μm samples. In such a thick GaN layer, i.e. a thick planar waveguide, the dispersion line for TE mode and for TM mode is theoretically close. Therefore, the ARPL spectrum of TE-TM state should present similar resonance peaks. However, these resonance peaks of TM-TE state were not observed as a TE-TM state. In addition, the resonance peak can be observed in samples regardless of whether the grating is coated with Ag or not. Thus, we think that this resonance might be due to the surface polariton resonance.

#136890 - $15.00 USD Received 19 Oct 2010; revised 9 Nov 2010; accepted 12 Nov 2010; published 22 Nov 2010

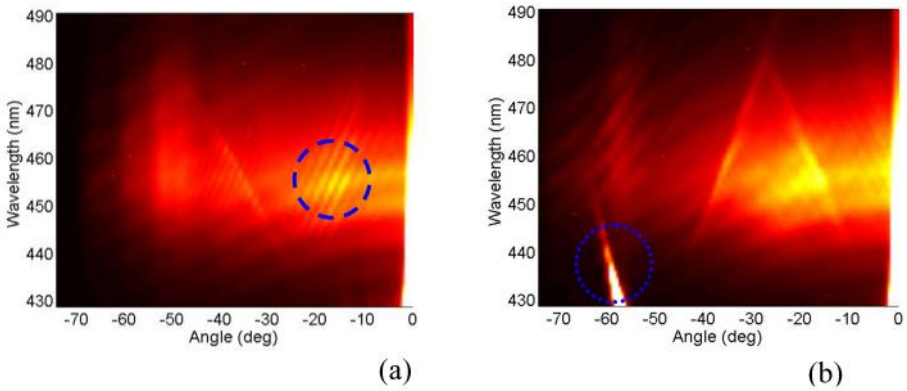


Fig. 6. TM-TE mode ARPL spectra of InGaN/GaN MQWs with 1D gratings without Ag coating for grating periods of (a) 0.3μm and (b) 0.5μm, respectively.

The blue dotted circle in Fig. 6(b) indicates the 405nm pumping source diffracted by the GaN grating. The plasmonic structure consists of two cascading metallic gratings. The gap between the two gratings is about 130nm. Therefore, the TE-polarized 405nm pumping source is cut-off. In addition the TM-polarized 405nm sample is attenuated as well. Owing to the fact that the sample with pure GaN grating lacks a metallic structure to reduce the background from the pumping source, the diffraction of the pumping source can be observed.

## 6. Conclusion

In this study, we investigate the polarization dependent ARPL spectra of InGaN/GaN QWs LED with two cascading plasmonic gratings. The plasmonic gratings consist of two Ag gratings with a half-pitch displacement. The ARPL spectra of the TE-TM state present broadband emission with resonance dips occasioned by the SP resonance. The TM-TE state presents resonance peaks with low sideband emission. All of these resonance properties can be tuned by modifying the geometric parameters of the plasmonic grating, especially the grating period. The ARPL spectrum of the LED sample with pure GaN 1D grating is also measured and discussed. The ARPL spectrum of the TM-TE state shows three kinds of resonance peaks, FP resonance, the guided-mode resonance and the surface polariton resonance. The investigated plasmonics LED represents resonance optical properties different from the conventional surface relief LED. They can be used in special applications, for example, for efficient angle-selected chromatic devices.

## Acknowledgements

The authors are grateful for the financial support of this research received from the National Science Council of Taiwan, R.O.C. under the grant number NSC98-2221-E-259-004- and 99-NU-E-259-001-.

#136890 - $15.00 USD Received 19 Oct 2010; revised 9 Nov 2010; accepted 12 Nov 2010; published 22 Nov 2010